

¹CR UK/MRC Oxford Institute for Radiation Oncology, Oxford, UK; ²PTCRI, University of Oxford, Oxford, UK; ³Radiation Oncology, Mayo Clinic, Rochester, MN, USA; ⁴King Saud University, Riyadh, Saudi Arabia.

Purpose/Objective:

More than half of cancer patients receive radiotherapy for radical or palliative purposes. Increasing survival rates in cancer patients make it important to study late side-effects, including secondary radiation-induced cancers. Although a number of predictive models exist, the absolute accuracy of these models in the radiotherapy dose range is limited partly due to scarcity of data and partly by extrapolation beyond historical data bounds. One of the challenges faced with applying models to the highly spatially varying dose distributions produced in modern radiotherapy is dose heterogeneity within organs of interest. The aim of this work is to investigate the difference between using mean dose (MD) and high-resolution voxel-by-voxel dose (VbV) maps for calculating malignant induction probability (MIP).

Materials & Methods:

A 3D conformal radiotherapy (3DCRT) and actively scanned proton plans were used for an adult patient and a teenage patient with medulloblastoma. MIP is calculated for each patient using the linear-quadratic (LQ), linear (LIN) and linear-no-threshold (LNT) models with in-house developed code. MIPs calculated using the mean dose to the organs as well as voxel-by-voxel dose are compared for individual organs and the whole body. A 3DCRT plan and an actively scanned proton therapy plan for an adult female MB patient were supplied by collaborators at Mayo Clinic. The prescribed dose was 36 Gy to the whole brain and spine with a 19.8 Gy boost to the posterior fossa (1.8Gy/fx).

All calculations are performed with a predefined priority list used to determine which structure each voxel is assigned to (and therefore which set of model parameters to apply). For VbV, the MIP was calculated using high-resolution dose maps that utilizes doses for each voxel, and for the mean dose, the mean dose of the whole organ was used to calculate MIP.

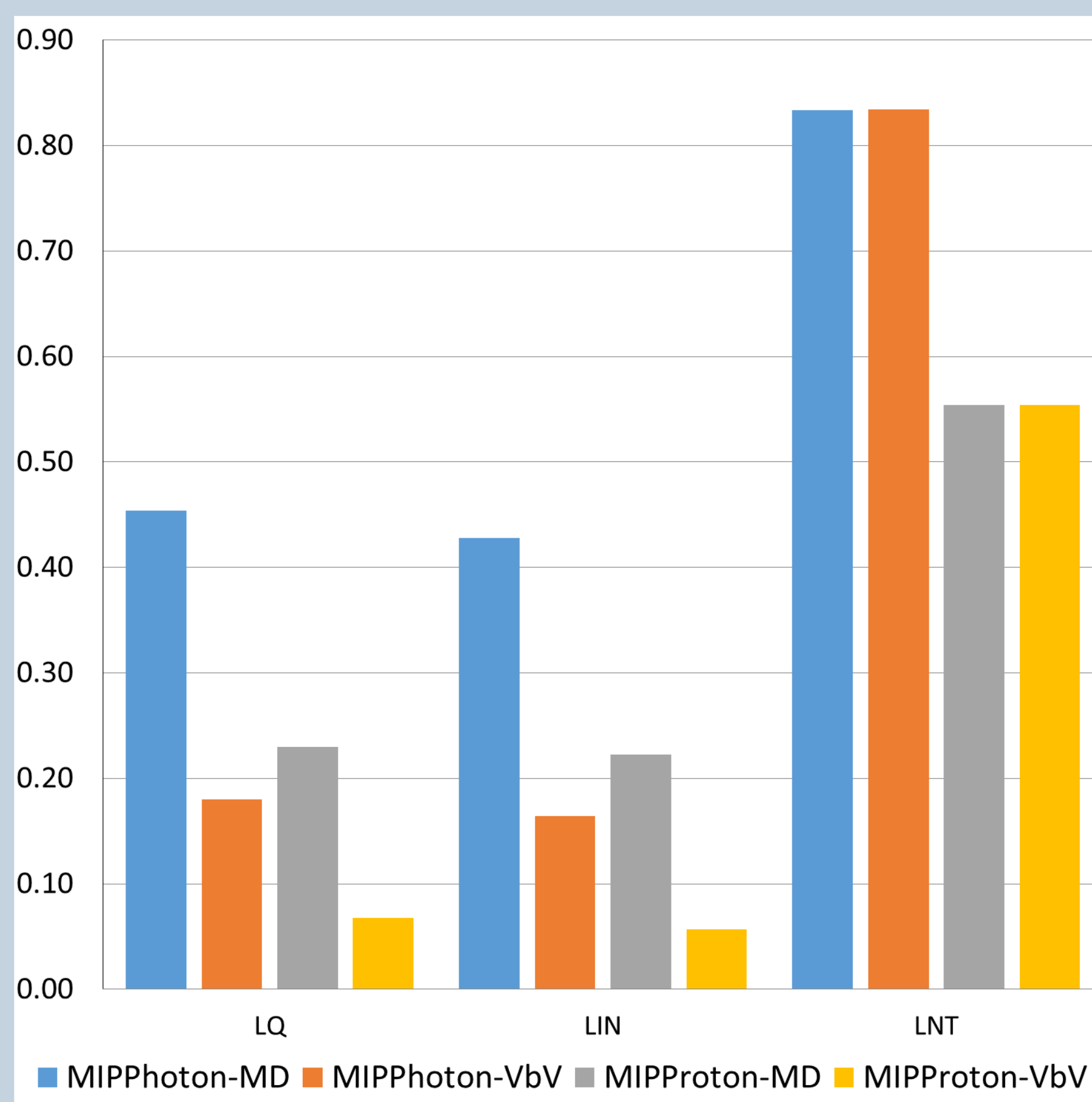


Figure 1: Teenage whole body MIP for the 3DCRT plan and proton plan using LQ, LIN and LNT models, using mean dose and VbV methods.

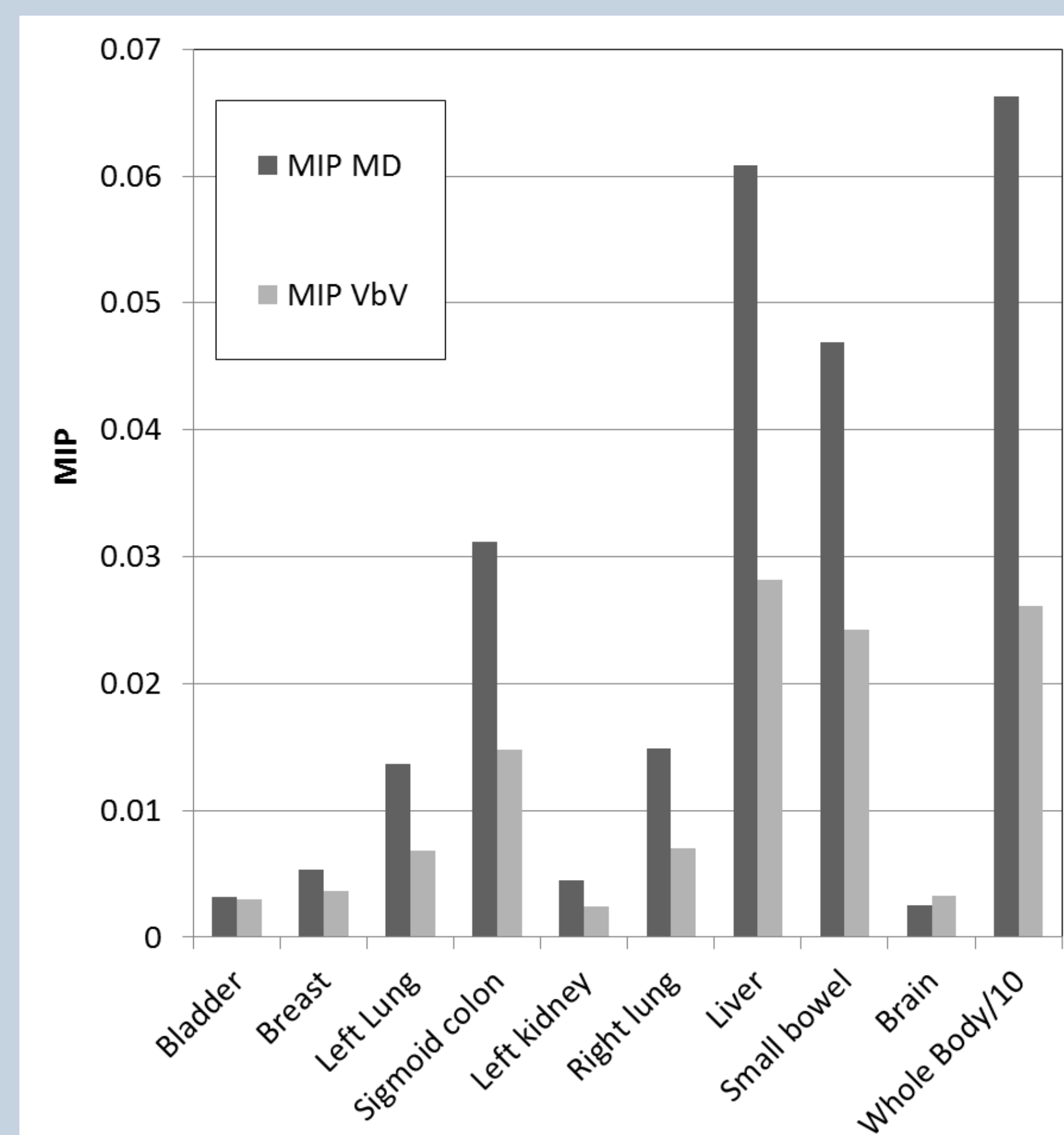


Figure 2: Adult MIP_{photon} (LQ) for selected organs & whole body using mean dose and VbV.

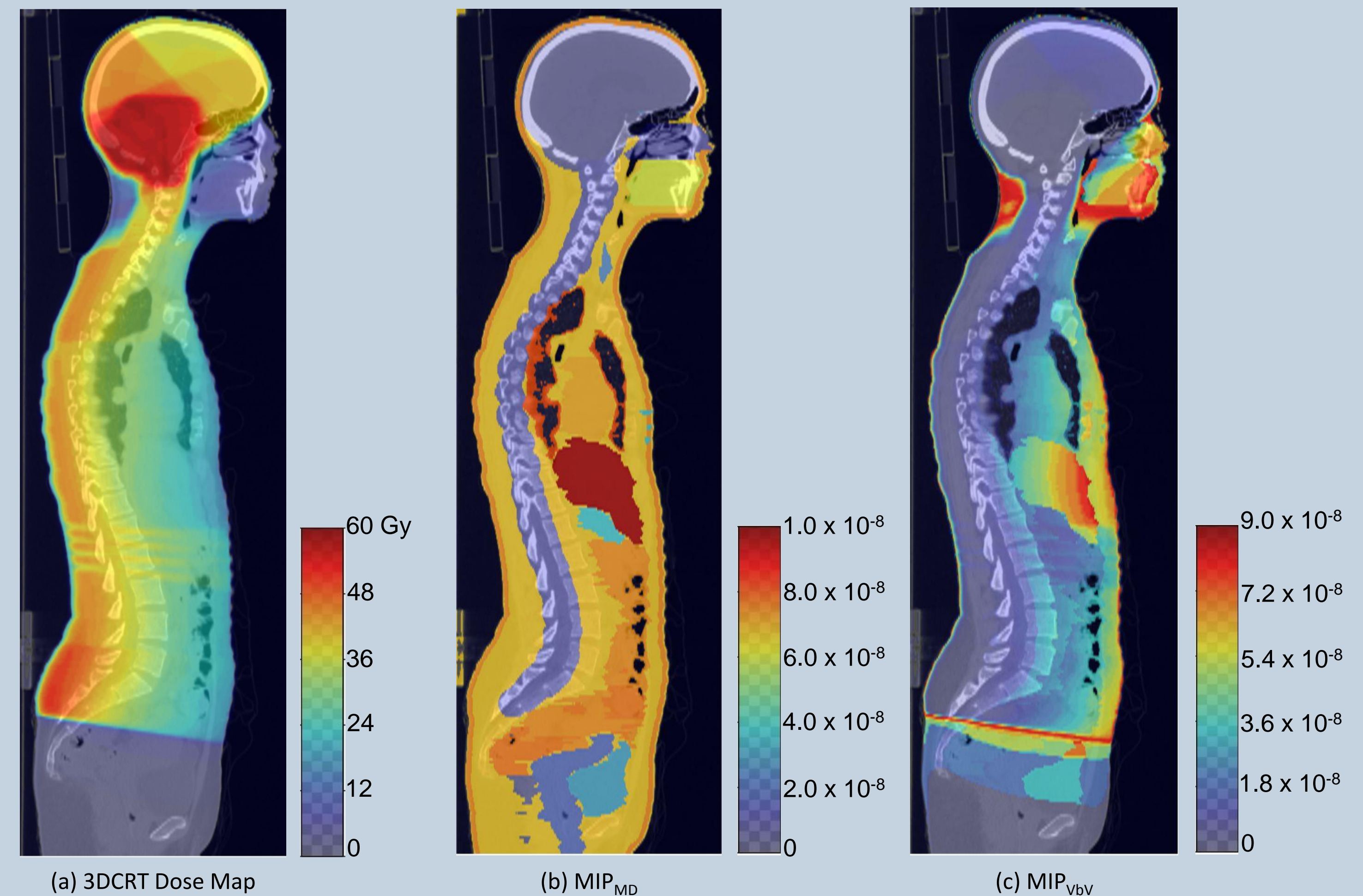


Figure 3: The 3DCRT plan for the adult patient (a), and the MIP map, calculated by the LQ model for the same patient using mean dose method (b) and VbV method (c). Note the heterogeneous dose deposition in some areas and the effect of that on the MIP produced using the two method.

Results:

Whole body MIP_{MD} for the adult patient photon plan was 0.663 (LQ), 0.637 (LIN), 0.929 (LNT), and 0.346 (LQ), 0.337 (LIN), 0.643 (LNT) for the proton plan. while MIP_{VbV} was 0.261 (LQ), 0.238 (LIN), 0.929 (LNT) for the photon plan, and 0.099 (LQ), 0.078 (LIN), 0.643 (LNT) for the proton plan.

Whole body MIP_{MD} for the teenage patient photon plan was 0.454 (LQ), 0.428 (LIN), 0.834 (LNT), and 0.229 (LQ), 0.222 (LIN), 0.554 (LNT) for the proton plan while MIP_{VbV} was 0.180 (LQ), 0.164 (LIN), 0.834 (LNT) for the photon plan, and 0.068 (LQ), 0.057 (LIN), 0.554 (LNT) for the proton plan.

For the LNT model, where MIP is linear with dose, the MD and VbV results are identical, as expected. For the nonlinear LQ and LIN models, significant differences in MIP can be seen (figure 1). Organ-specific MIPs vary over a wide range (figure 2), although MIP_{MD} is higher than MIP_{VbV} by an average factor of 1.7 (adult) and 1.6 (teenage) for both the LQ and LIN models for 3DCRT plans and an average factor of 3.1 (adult) and 2.3 (teenage) for proton plans. Use of MD gives consistently higher MIP estimates than VbV calculation in areas of dose heterogeneity (note reversal of this trend in the brain, which has a uniform high dose).

Conclusions:

Results demonstrate large systematic differences between the risk estimates produced using either mean dose or voxel-by-voxel calculation. Although the relative relation between MIP_{photon} and MIP_{proton} remains broadly constant, using mean dose in heterogeneous dose distributions potentially overestimates MIP and, by association, secondary cancer risk. This should be taken in consideration when designing studies of secondary cancer risk (figure 3).

*MIP Models used: The linear-quadratic malignant induction model (LQ): $MIP = n (\gamma d + \delta d^2) e^{-n(\alpha d + \beta d^2)}$, The linear malignant induction model (LIN): $MIP = \mu D e^{-n(\alpha d + \beta d^2)}$, Linear-no-threshold malignancy induction model (LNT): $MIP = \mu D$, Linear-with-threshold malignancy induction model.

SF: the surviving fraction of cells given in (*n*) fractions of dose (*d*). **α** and **β**: the radiosensitivity parameters, are the linear and quadratic component of the curve, respectively. **γ** and **δ**: the malignant induction coefficients. **μ**: linear coefficient, **D** is the total dose.

Acknowledgment : This work was done with generous support from King Saud University (Riyadh, Saudi Arabia), CR UK and MRC.